International Journal of Nanomedicine

Dovepress
open access to scientific and medical research

Open Access Full Text Article

ORIGINAL RESEARCH

Indocyanine Green-Parthenolide Thermosensitive Liposome Combination Treatment for Triple-Negative Breast Cancer

This article was published in the following Dove Press journal:
International Journal of Nanomedicine

Xin Jin[1,2]
Xinyue Lu[3]
Zhenhai Zhang[4]
Huixia Lv[3]

[1]Department of Hospital Pharmacy, Suqian First Hospital, Suqian 223800, People's Republic of China; [2]Department of Pharmaceutics, Suqian Clinical College of Xuzhou Medical University, Suqian 223800, People's Republic of China; [3]Department of Pharmaceutics, State Key Laboratory of Natural Medicines, China Pharmaceutical University, Nanjing 210009, People's Republic of China; [4]Jiangsu Province Hospital on Integration of Chinese and Western Medicine Affiliated with Nanjing University of Chinese Medicine, Nanjing 210000, People's Republic of China

Background: Certain patients with triple-negative breast cancer cannot tolerate the serious adverse effects of cytotoxic chemotherapy agents, which significantly affect the disease prognosis.
Purpose: Research into the combined use of photosensitizers and non-cytotoxic antineoplastic drugs for the safe treatment of triple-negative breast cancer is vital.
Methods: In this study, the photosensitizer indocyanine green and the natural drug parthenolide were co-loaded into thermosensitive liposomes. Under a near-infrared irradiation, indocyanine green reached excitation levels, releasing heat, and the liposome underwent a phase transition, releasing the drug were researched.
Results: Thus, indocyanine green and parthenolide exert synergistic antineoplastic effects. In the nude mice xenograft MDA-MB-231 tumor model, the tumor inhibition rate of indocyanine green-parthenolide thermosensitive liposomes was approximately 2.08-fold than that of paclitaxel and demonstrated a good initial safety evaluation.
Conclusion: Photosensitizers and non-cytotoxic antineoplastic agents in combination with nanoscale carriers should be further investigated for the treatment of tumors.
Keywords: indocyanine green, parthenolide, thermosensitive liposomes, triple-negative breast cancer, chemo-photothermal synergetic therapy

Background

Breast cancer is a malignancy that threatens the safety and health of women. It accounts for approximately 30% of the neoplasms in women, and the associated mortality rate is as high as 24%.[1] Triple-negative breast cancer is a special subtype of breast cancer, which is negative for expressions of the estrogen receptor, the progesterone receptor, and the human epidermal growth factor receptor and accounts for approximately 15–20% of all the breast cancer cases.[2] Triple-negative breast cancer has a high incidence of visceral metastasis and early recurrence compared to other phenotypes.[3] Recently, atezolizumab plus nab-paclitaxel has been chosen to treat metastatic triple-negative breast cancers.[4,5] Among patients with the PD-L1–positive tumors, the median overall survival was 25 months. However, adverse events that led to the discontinuation of this treatment occurred in 15.9% of the patients.[5] Therefore, it is necessary to find alternative drug treatments that are safe and effective.

The combined administration of the non-cytotoxic drugs has better antitumor effects. Lee et al used a combination of metformin and hemin to treat triple-negative breast cancer, and the combination effectively controlled tumor growth by inhibiting the mitochondrial metabolism.[6] Yamamoto et al found that palbociclib and MLN0128 have a synergistic

Correspondence: Zhenhai Zhang; Huixia Lv
Tel +8618913823932; +8613912965842
Email david23932@163.com; lvhuixia@163.com

submit your manuscript | www.dovepress.com
DovePress
http://doi.org/10.2147/IJN.S245289

anticancer activity against triple-negative breast cancer, and the combination therapy exerted better inhibitory effects on tumor growth than those seen with control or monotherapy.[7]

In recent years, photothermal/photodynamic therapy has received widespread attention in the field of breast cancer treatment. The use of near-infrared light to trigger photosensitizers enables the control of killing tumor cells. Compared to the traditional chemotherapy, the photothermal/photodynamic therapy decreases systemic toxicity and the risk of drug resistance.[8] Indocyanine green (ICG), is an FDA-approved photosensitizer, widely used in the clinical diagnosis of liver diseases, macular hole surgery, tissue perfusion, and lymph node localization, and is safe.[9] In cancer diagnosis and treatment, ICG can be used, not only for a near-infrared fluorescence/photoacoustic dual-modality imaging, but also for a photodynamic/photothermal synergistic therapy. Irradiated ICG with near-infrared light converts light energy into heat energy and singlet oxygen to kill tumor cells.[10] However, the clinical application of ICG has limitations such as; a short serum half-life, a low tissue permeability, and poor targeting of tumor tissues. There are several reports on the use of tumor-targeting carriers loaded with ICG. Thermosensitive liposomes can respond to the photothermal effects of the photosensitizer, promoting the transformation of the carrier from the colloidal crystal state to the liquid crystal state, increasing its fluidity and permeability. This allows the drug to diffuse across the membrane into tissues in large amounts, thus forming aggregates with high concentration in the tumor site and has good prospects for clinical applications.[11] There are several reports that describe loading photosensitizers and cytotoxic drugs into the nanoscale-targeted carriers simultaneously to improve the efficacy of photosensitizers for the treatment of triple-negative breast cancer, such as platelet biomimetic nanoparticles, perfluorocarbon double nanoemulsions, and hybrid bicelles.[12–14] However, there are only a few studies on the use of photosensitizers and non-cytotoxic antineoplastic agents for the treatment of triple-negative breast cancer, highlighting the need for further research.

Parthenolide (PTL) is a sesquiterpene lactone isolated from Asteraceae that has antitumor effects on breast, lung, and liver cancers. It is safe and is gradually receiving attention as a potential treatment.[15,16] The key mechanisms of action of PTL are the induction of reactive oxygen species (ROS) and the impairment of mitochondrial membrane potential (MMP). However, because PTL does not readily dissolve in water, it is rapidly metabolized in the body and has a short half-life, and its antitumor effect needs to be improved. In this study, ICG and PTL were co-loaded into thermosensitive liposomes and used in combination to treat triple-negative breast cancer with targeted drug delivery. ICG in thermosensitive liposomes responded to a near-infrared light irradiation, and increased drug concentration in tumor cells; thereby, exerting the synergistic effect in the treatment of triple-negative breast cancer (as shown in Scheme 1).

Methods

Materials

Dipalmitoylphosphatidylcholine (DPPC), distearoylphosphatidylcholine (DSPC), and cholesterol were obtained from A.V. T. Pharmaceutical Co., Ltd (Shanghai, China). Parthenolide was purchased from Chengdu Dexter Biotechnology Co., Ltd (Chengdu, China). Indocyanine green was bought from Shanghai Ziyi Reagent Factory (Shanghai, China). The L-15 culture medium, fetal bovine serum (FBS), phosphate-buffered solution (PBS), 4′,6-diamidino-2-phenylindole (DAPI), 3-(4,5-dimethyl-2-thiazolyl)-2,5-diphenyl-2-H-tetrazolium bromide (MTT), and relevant reagent kits were obtained from Nanjing KeyGen Biotech Co., Ltd (Nanjing, China).

Cells and Animals

MDA-MB-231 cell line was bought from Nanjing KeyGen Biotech Co., Ltd. It was cultivated in the L-15, supplemented with FBS (10%, v/v) at 37°C under humidified conditions with 5% CO_2.

Female BALB/c nude mice were provided by the Qinglongshan Animal Breeding Farm and reared under aseptic conditions. Animal welfare and experimental procedures were strictly in accordance with the Guide for the Care and Use of Laboratory Animals (US National Research Council, 1996) and the related ethics regulations of the Suqian First Hospital. Animal protocols were reviewed and approved by the internal animal care and use committee of the Suqian First Hospital.

Preparation of the PI-TSL

PI-TSL was obtained using the thin-film hydration method, and in accordance with previous reports.[17,18] DPPC, DSPC, cholesterol, ICG, and PTL (200:50:50:1:15.3, w/w) were dissolved in a solution of chloroform and methanol (3:1, v/v) in a round bottom flask and subsequently evaporated using a rotary evaporator at 40°C followed by overnight drying under vacuum. The resultant film was hydrated with ultrapure water at 55°C for 1 h. The obtained solution was then dispersed using an ultrasonic probe and filtered to obtain the PI-TSL. The PTL-TSL was prepared in the absence of ICG following the same method described above.

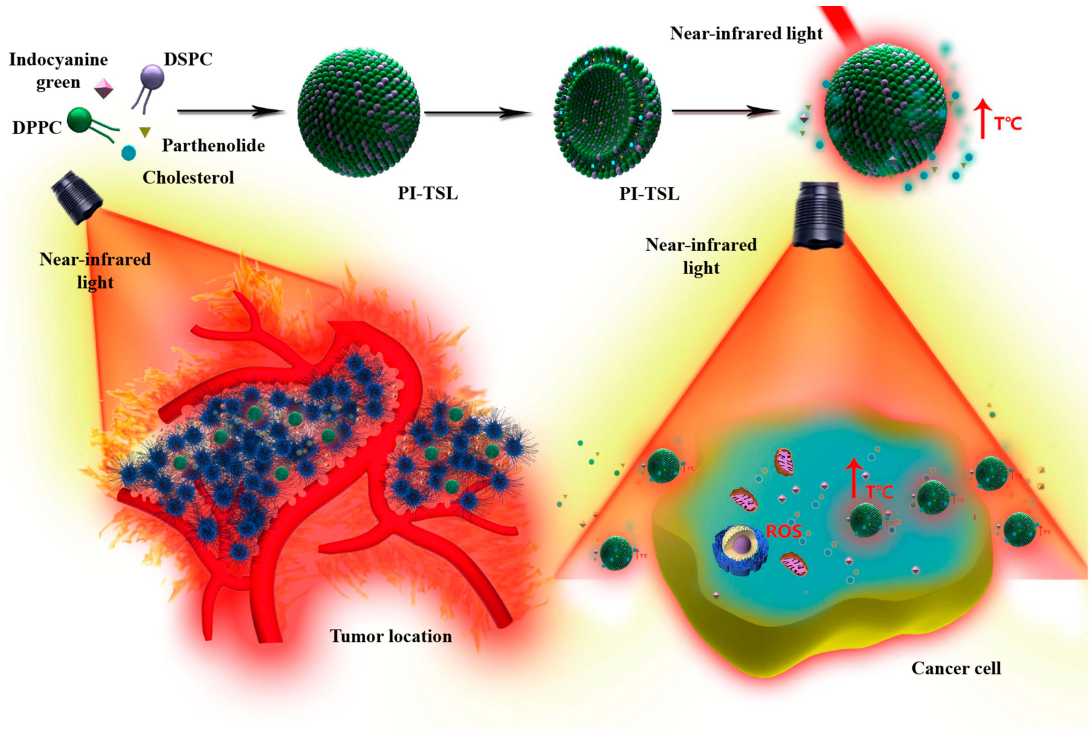

Scheme 1 Thermosensitive liposomes responded to a near-infrared light irradiation, and exerted the synergistic effect in the treatment of triple-negative breast cancer.

Characterization of the PI-TSL

Particle size distribution, the ζ potential, and morphology of the PI-TSL were characterized. The hydrodynamic size and the ζ potential were evaluated using a dynamic light-scattering instrument (Zetasizer, Malvern, UK). All liposome dispersions were diluted with distilled water (1:100) prior to the characterization of particles.

The morphology of PI-TSL was analyzed by transmission electron microscopy (TEM, JEM-Z300FSC, JEOL, Japan). A 100-fold diluted dispersion of the liposomes in distilled water was mounted on a carbon grid. The dispersion was stained with uranyl acetate solution for 1 min. Excess stain was removed using filter paper, and the sample was left to be air-dried.

The entrapment efficiencies (EE) and the drug loading (DL) values were calculated as follows:

EE (%) = mass of a drug in the liposomes/mass of this drug loaded initially × 100

DL (%) = mass of all drugs in the liposomes/mass of liposome ×100

Analysis of the Near-Infrared Light Response (NIR)-Triggered Drug Release in vitro

To evaluate the drug release behavior, 2 mL of the aqueous dispersion of PTL-TSL (+), PI-TSL (-), or PI-TSL (+) was loaded into dialysis bags and placed in 200 mL of PBS (containing 1% SDS) at 37°C. With gentle shaking, 1 mL of the releasing medium was obtained at different time points. For the PTL-TSL (+) and PI-TSL (+) groups, the dialysis bag was exposed to a laser (808 nm, 0.5 W/cm^2) for 5 min before collecting the dissolution media.

Photothermal Effect in vitro

To examine the photothermal effect in vitro, water, ICG (20 μg/mL), and PI-TSL (ICG 20 μg/mL) were exposed to 808 nm laser with 0.5 W/cm^2 for 5 min. The temperatures were then recorded using a thermal imaging camera (Tis75; Fluke, Germany).

Cytotoxicity Analysis of the PI-TSL

The MDA-MB-231 cells were seeded in 96-well plates with the L-15 culture medium containing 10% FBS and incubated at 37°C under 5% CO_2 for 24 h. The cells were then treated with different formations (as shown in Figure 1A) for 4 h with or without laser irradiation (808 nm, 0.5 W/cm^2 for 5 min). To determine the viability of cancer cells, followed by re-incubation at 37°C for 24 h, MTT was added to each well with L-15, incubated for 4 h, and measured using a microplate reader (Multiskan Sky, Thermo Fisher, American).

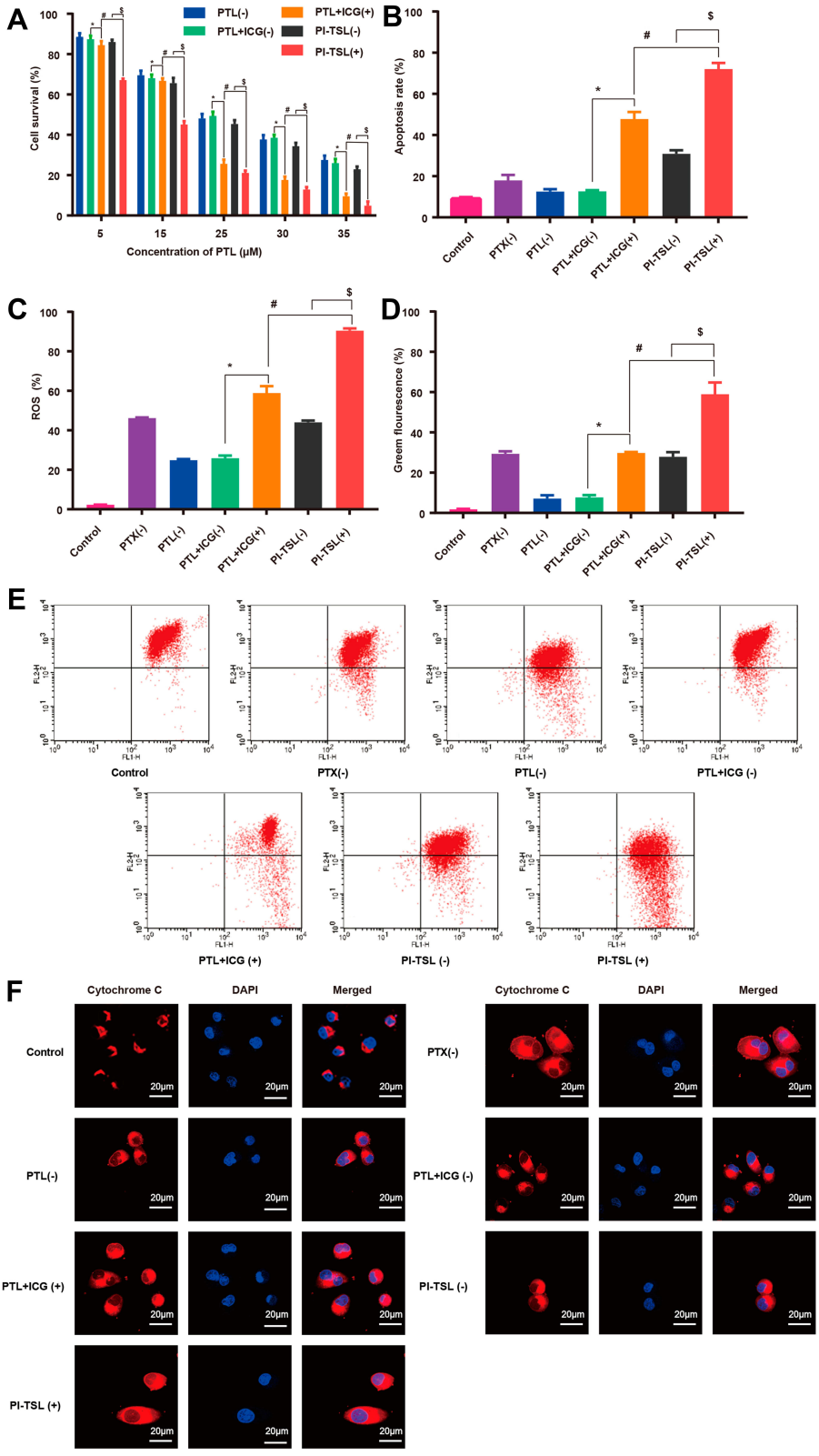

Figure 1 Cytotoxicity (**A**), induced apoptosis (**B**), reactive oxygen species (**C**), mitochondrial membrane potential (**D** and **E**), and cytochrome c release (**F**) under different conditions in vitro. *Stands for $P < 0.05$ for ICG+PTL (-) versus ICG+PTL (+) at same concentration; #stands for $P < 0.05$ ICG+PTL (+) versus PI-TSL (+) at same concentration; $stands for $P < 0.05$ PI-TSL (-) versus PI-TSL (+) at same concentration.

Induction of Apoptosis by Reactive Oxygen Species

The MDA-MB-231 cells were seeded in 24-well plates at a density of 5×10^3 cells/well and cultured overnight. To determine the apoptotic effect, the cells were irradiated with 0.5 W/cm^2 laser beam at 808 nm for 5 min or were left untreated after 4 h of incubation with the normal culture medium (control), 80 nM PTX (-), 25 μM PTL (-), 25 μM PTL+2.5 μM ICG (-), 25 μM PTL+2.5 μM ICG (+), PI-TSL (-) containing 25 μM PTL and 2.5 μM ICG, or PI-TSL (+) containing 25 μM PTL and 2.5 μM ICG. Following this, the cells were cultured for a further 24 h. The cells were analyzed using an apoptosis assay kit, reactive oxygen species (ROS) activity assay kit, and mitochondrial membrane potential (MMP) detection kit by flow cytometry (Beckman Coulter, Brea, American).

After treatment, the cells were incubated with 50 μL of anti-cytochrome c antibody (1:50) for 2 h, followed by 50 μL of the TRITC-conjugated secondary antibody (1:100) and stained for 1 h. Cancer cell nuclei were then stained using DAPI for 5 min in dark and observed using a confocal laser scanning microscope (CLSM).

Invasion Assay

Invasion assays were performed using cell culture inserts covered with Matrigel. After treating the cells with the normal culture medium (control), 80 nM PTX (-), 25 μM PTL (-), 25 μM PTL+2.5 μM ICG (-), 25 μM PTL+2.5 μM ICG (+), PI-TSL (-) containing 25 μM PTL and 2.5 μM ICG, or PI-TSL (+) containing 25 μM PTL and 2.5 μM ICG for 24 h, 1×10^5 cells were added to the upper chamber containing a serum-free L-15. The bottom chamber was filled with L-15 containing 10% FBS. Invading cells on the lower surface of the filter were stained with 0.1% crystal violet and photographed. The mean number of cells from six fields of three separate trials was used to calculate the average number of migratory cells.

Cell Cycle Analysis

The MB-231 cells were harvested with trypsin after exposure to the normal culture medium (control), 80 nM PTX (-), 25 μM PTL (-), 25 μM PTL+2.5 μM ICG (-), 25 μM PTL+2.5 μM ICG (+), PI-TSL (-) containing 25 μM PTL and 2.5 μM ICG, or PI-TSL (+) containing 25 μM PTL and 2.5 μM ICG for 24 h. After washing twice with chilled PBS, the cells were fixed in 70% ethanol and stored at 4°C for 12 h. Before analyzing the DNA content, the samples were resuspended in 1.0 mL of a hypotonic solution of propidium iodide (PI) (50 mg/mL PI, 0.1 mg/mL RNase A, and 0.2% Triton X-100), and incubated in the dark for 30 min prior to flow cytometry.

Cellular Uptake in vitro

The MB-231 cells were cultured in 2-cm glass dishes for 24 h. The culture medium was replaced with a serum-free medium containing ICG (-), PTL+ICG (-), and PI-TSL (-) with 2.5 μM ICG and then cultured at 37°C for 1 h and 4 h periods. DAPI was added after observing the cells. The cells were washed with PBS three times and observed using a CLSM. The fluorescence intensity at 4 h was quantitatively analyzed using flow cytometry.

Targeting Effect and Biodistribution in vivo

The MDA-MB-231 cells (5×10^6/mL) were collected in a serum-free L-15 medium (200 μL), and subcutaneously injected into the right forelimb axilla of female BALB/c nude mice. After two weeks, when the tumor volume had increased to 400 mm^3, the mice were intravenously injected with 2 mg/kg ICG (+) or PI-TSL (+) containing 30 mg/kg PTL and 2 mg/kg ICG via the lateral tail vein. Fluorescence images of the mice were captured at 1 h, 4 h, 8 h, 12 h, and 24 h post-injection. Images of the excised major organs and tumors were also captured ex vivo.

Photothermal Imaging in vivo

The MDA-MB-231 cells (5×10^6/mL) were collected in a serum-free L-15 medium (200 μL) and subcutaneously injected into the right forelimb axilla of female BALB/c nude mice. After two weeks, the nude mice bearing MDA-MB-231 tumors were injected with physiological saline, 2 mg/kg ICG (+), and PI-TSL (+) containing 30 mg/kg PTL and 2 mg/kg ICG via the tail vein, as the tumor volume had reached approximately 400 mm^3. After 8 h of incubation, the tumor tissues were irradiated with a laser beam for 5 min. The temperature of the tumor region was obtained using an infrared thermal imaging camera (Tis75, Fluke, Germany).

Analysis of Therapeutic Effect on Xenograft Model in vivo

The MDA-MB-231 cells (5×10^6/mL) were collected in a serum-free L-15 medium (200 μL) and subcutaneously injected into the right forelimb axilla of female BALB/c nude mice. After one week, nude mice bearing a MDA-MB-231 tumor with a volume of approximately 120 mm^3 were randomly divided into six groups and injected with saline,

10 mg/kg PTX, 30 mg/kg PTL+ 2 mg/kg ICG (-), 30 mg/kg PTL+ 2 mg/kg ICG (+), PI-TSL (-) containing 30 mg/kg PTL and 2 mg/kg ICG, or PI-TSL (+) containing 30 mg/kg PTL and 2 mg/kg ICG via the tail vein every two days for 19 consecutive days. Both, the tumor volume and the body weight of the mice were examined every two days. The mice were sacrificed at the end of the experiment and the major organs and tumors were harvested. The samples were collected and stained with hematoxylin-eosin staining (H&E) for analysis. Tumor tissues were further subjected to immunohistochemistry for Ki67 evaluation.

Statistical Analysis

The data have been expressed as mean ± standard deviations. Statistical significance of differences between experimental groups was calculated using GraphPad Prism (version 7.00, GraphPad Software). For single comparisons, a two-tailed Student's *t*-test was used. For multiple comparisons, the Tukey's post hoc tests, and one-way ANOVA were performed. Statistical significance between the results was determined using $P < 0.05$.

Results

Characteristics of the PI-TSL

The hydrodynamic size of PI-TSL was 150.4 nm±9.1 nm (Figure 2A) with −4.6 mV±0.32 mV ζ potential and a low polydispersity index (PDI=0.184±0.015), as determined by using the a dynamic light scattering method. For the PI-TSL, we observed entrapment efficiencies of 92.99% ±3.58% and 94.94%±2.69%, and drug-loading efficiencies of 4.43%±0.29% and 0.302%±0.022% for PTL and ICG, respectively. The concentration of ICG and parthenolide in liposomes was 0.202 mg/mL and 3.06 mg/mL, respectively. Morphological observations revealed that the PI-TSL was spherical with a uniform size distribution (Figure 2B). However, the size observed using TEM was smaller than that of the hydrodynamic size, which may be due to the different detection methods. For the hydrodynamic size, there is a hydration layer outside the particle. The hydration layer is included in the measurement. For transmission electron microscopy (TEM) measurements, only the dry particle size is considered. The absence of a hydration layer results in the observation of a smaller size when using the TEM compared to the size observed based on hydrodynamics.

Both the PTL-TSL (+) and the PI-TSL (-) demonstrated a low release concentration of PTL (Figure 2C). For the PTL-TSL (+), the absence of ICG eliminated heat generation, resulting in a low release rate. The PI-TSL (+) and the PI-TSL (-) were irradiated in an on-off pattern, resulting in a final PTL release of 90%±5.69% for the PI-TSL (+) at 4 h, which was considerably higher than that without an NIR irradiation of the PI-TSL (-) ($P < 0.05$). It can be concluded that the PI-TSL exhibits an excellent NIR-response and may induce low adverse effects in healthy tissues. Furthermore, after 5 min of laser irradiation, the temperature of water, ICG (+), and PI-TSL (+) was 28.8°C±1.9°C, 42.1°C±3.2°C, and 48.2°C±3.5°C, respectively (Figure 2D).

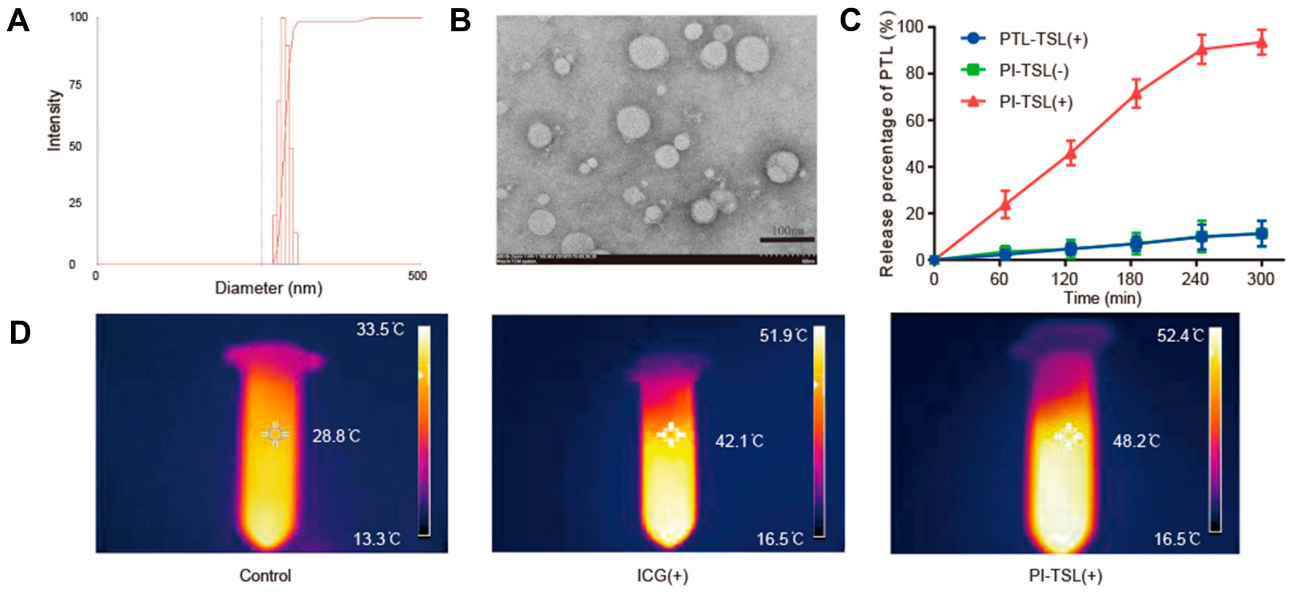

Figure 2 Hydrodynamic size (**A**) and morphology (**B**) of PI-TSL. In vitro NIR-triggered drug release (**C**) and photothermal effects (**D**) of different formations.

Antitumor Efficacy in vitro

No significant differences in cell viability were observed between the PTL (-) and the PTL+ICG (-) at the same concentration of PTL ($P > 0.05$). The ICG without the NIR laser excitation cannot convert heat to improve the antitumor effect. However, the PTL+ICG (+) treatment with 0.5 W/cm^2 laser irradiation for 5 min exhibited a significantly enhanced cytotoxicity compared to that observed with the PTL+ICG (-) at the same concentration ($P < 0.05$). The anti-tumor efficiency of the PTL+ICG (+) increased by 23.5% with 35 μM PTL compared to that observed with the PTL+ICG (-) ($P < 0.05$). The cell viability for both the PTL+ICG (+) and the PTL +ICG (-) was very low. This may be because both the PTL+ICG (+) and the PTL+ICG (-) were studied in the presence of a high concentration of PTL (35 μM). As shown in Figure 1A, the cell viability for PTL at 35 μM was only 27.5%. Furthermore, ICG absorption of the NIR laser converts heat to improve the efficiency of antitumor therapy. Therefore, the PTL+ICG (+) had a better antitumor effect than that of the PTL+ICG (-) ($P < 0.05$) and the cell viability of the PTL+ICG (+) and the PTL+ICG (-) was low. Meanwhile, the survival rate of the MDA-MB-231 cells treated with the PI-TSL (+) gradually decreased as the concentration increased, and presented the maximum anti-tumor effect compared with that of the other groups. In the PI-TSL (+) group, at 35 μM PTL, the cell survival rate was only 5.68%±0.71%. These results suggest that thermosensitive liposomes may be capable of promoting an uptake of the PTL and the ICG aggregates at the tumor cells. Consequently, we concluded that combination therapy involving thermosensitive liposomes results in a significantly improved the therapeutic efficiency compared with that of the chemo-photothermal synergetic therapy (Figure 1A) ($P < 0.05$).

Induction of Apoptosis by Reactive Oxygen Species

As shown in Figure 1B, after treatment with the PTL+ICG (+) containing 25 μM PTL and 2.5 μM ICG, 47.82%±3.77% of the cells were apoptotic, and 12.56%±1.58% cells were apoptotic in the PTL+ICG (-) group at the same concentration. With the PI-TSL (+) treatment, the apoptosis rate increased 1.51-fold compared to that with the PTL+ICG (+) treatment ($P < 0.05$). At the concentration of 25 μM PTL and 2.5 μM ICG, treatment with the PTL+ICG (+) (Figure 1C) increased ROS generation compared to that observed with the treatment of PTL+ICG (-) ($P < 0.05$). Highest ROS generation was observed in the PI-TSL (+) treatment. Following treatment with the PI-TSL (+), ROS generation increased by 53.57% compared to that in the PTL +ICG (+) group ($P < 0.05$). Excessive ROS impairs MMP. Red fluorescence gradually changed to green fluorescence, indicating a decrease in the MMP. The results of MMP (Figure 1D and E) were consistent with the data from the ROS results described above. Induced ROS generate abundant amounts of oxygen radicals. The mitochondrial membrane is primarily composed of polyunsaturated fatty acids. Free oxygen radicals have a high affinity to the unsaturated bonds of poly-unsaturated fatty acids. This may cause lipid peroxidation in the mitochondrial membrane. As a result, the structure and function of the mitochondrial membrane is altered, which may increase permeability, and consequently, decrease the mitochondrial membrane potential (MMP). The differences observed in the cytochrome between the controls and the other samples at the concentration of 25 μM PTL and 2.5 μM ICG have been shown in Figure 1F. These results were consistent with the data described above.

After a combined administration (Figure 1), the in vitro IC_{50} value decreased by 26.8%, especially after treatment with a near-infrared light for the PI-TSL (+), compared with that observed with the PTL+ICG (+) group ($P < 0.05$). The apoptosis rate and oxidative stress levels of PI-TSL (+) increased by 2.81- and 1.37-fold ($P < 0.05$), respectively, in comparison to that observed with the PTL (-) at the concentration of 25 μM PTL treatment. Such significantly enhanced oxidative stress and induction of local hypoxia, starvation, DNA cross-linking, and strand breakage tend to kill the tumor cells.[19] In addition, the increased local temperature also leads to deformities in protein folding, resulting in DNA damage and denaturation,[20] which further exert anti-tumor effects.

Invasion Assay

Transwell assays were employed to estimate the cell migration and metastasis abilities. The number of cancer cells passing through the transwell membrane filter decreased to 16.5% in the PI-TSL (+) group at the concentration of 25 μM PTL and 2.5 μM ICG compared to that observed in the control groups (Figure 3A) ($P < 0.05$). These results indicate that the PI-TSL (+) inhibits the invasion ability of the malignant MDA-MB-231 cells.

Cell Cycle Arrest

Cell cycle progression is a hallmark of cell proliferation. As shown in Figure 3B, PTL (-), PTL+ICG (-), PTL+ICG (+), PI-TSL (-), and PI-TSL (+) at the concentration of 25 μM of PTL were capable of arresting the cancer cell cycle in the S phase compared to that observed in the control. The PI-TSL (+) had the strongest effect on the cell cycle arrest. Noteworthy, the parthenolide-induced G0/G1 phase cell cycle arrest and the G2/M arrest was observed in the MCF7 cell line[21] and the SH-J1 cells,[22] respectively. A previous study has indicated that

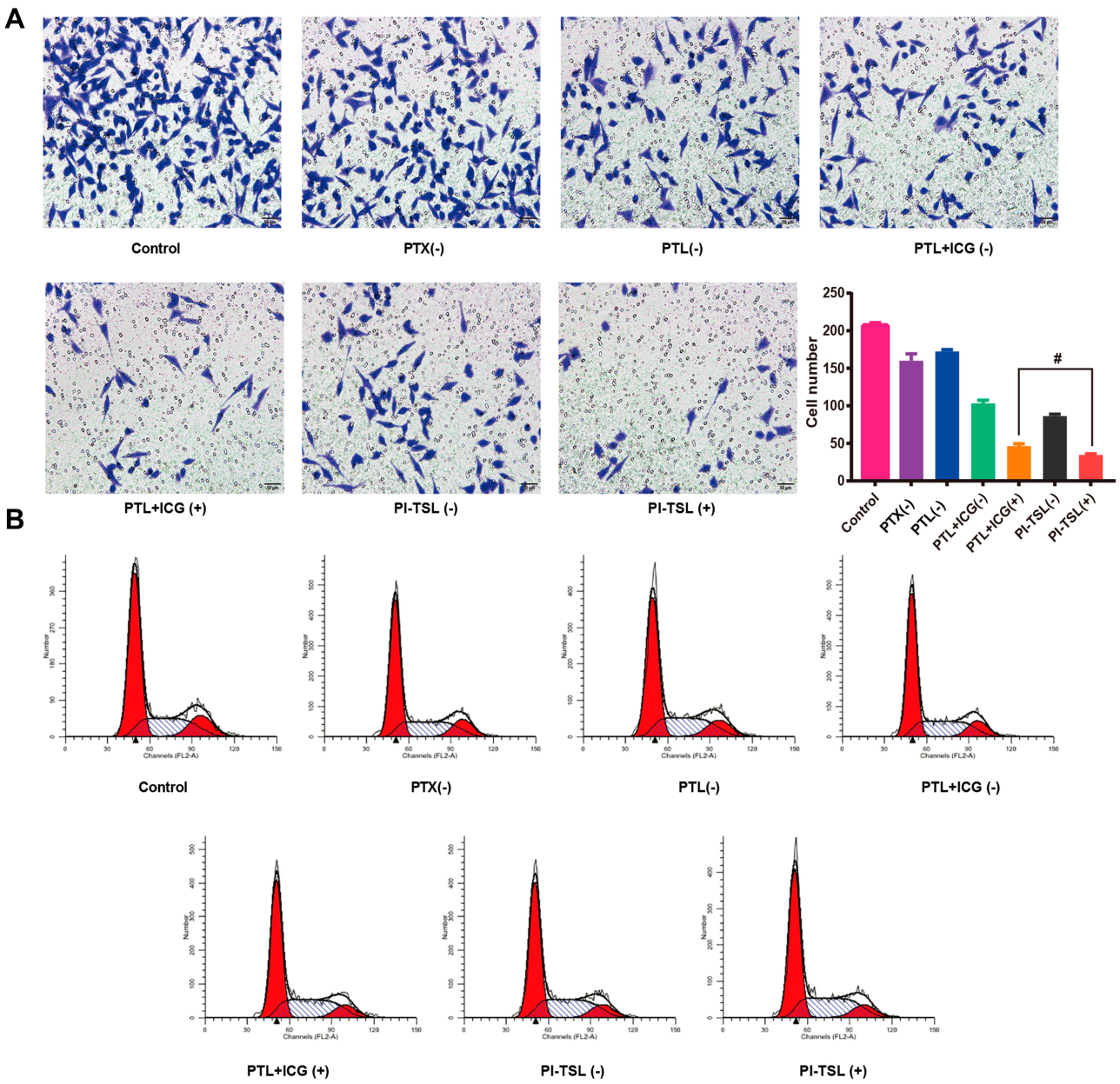

Figure 3 Invasion inhibition assay (**A**) and cell cycle arrest effect (**B**) of different formations under various conditions. #Stands for P < 0.05 ICG+PTL (+) versus PI-TSL (+).

a phase-dependent cell cycle arrest through parthenolide is cell-type specific, while PTX (-) mainly affects the microtubule formation that increases the G2/M cell population, as shown in our previous study.[23]

Cellular Uptake

As shown in Figure 4A, the red fluorescence intensity of ICG (-) at the concentration of 2.5 μM ICG was relatively low in all the groups at 1 h. With increase in time, the uptake of ICG (-) increased. After incubation for 4 h, an intense red fluorescence was observed in the PI-TSL (-)-treated group than that observed in the groups treated with ICG (-) and PTL +ICG (-) at an equal concentration of 2.5 μM ICG. For quantitative analysis (Figure 4B), the MDA-MB-231 cells absorbed considerably more ICG for the PI-TSL (-) group with 2.5 μM ICG, 2.22- and 1.61-times higher than that of the counterparts exposed to ICG (-) and PTL+ICG (-) at 4 h incubation period ($P < 0.05$). The results indicate that thermosensitive liposomes are capable of promoting the uptake of loaded drugs without a laser trigger.

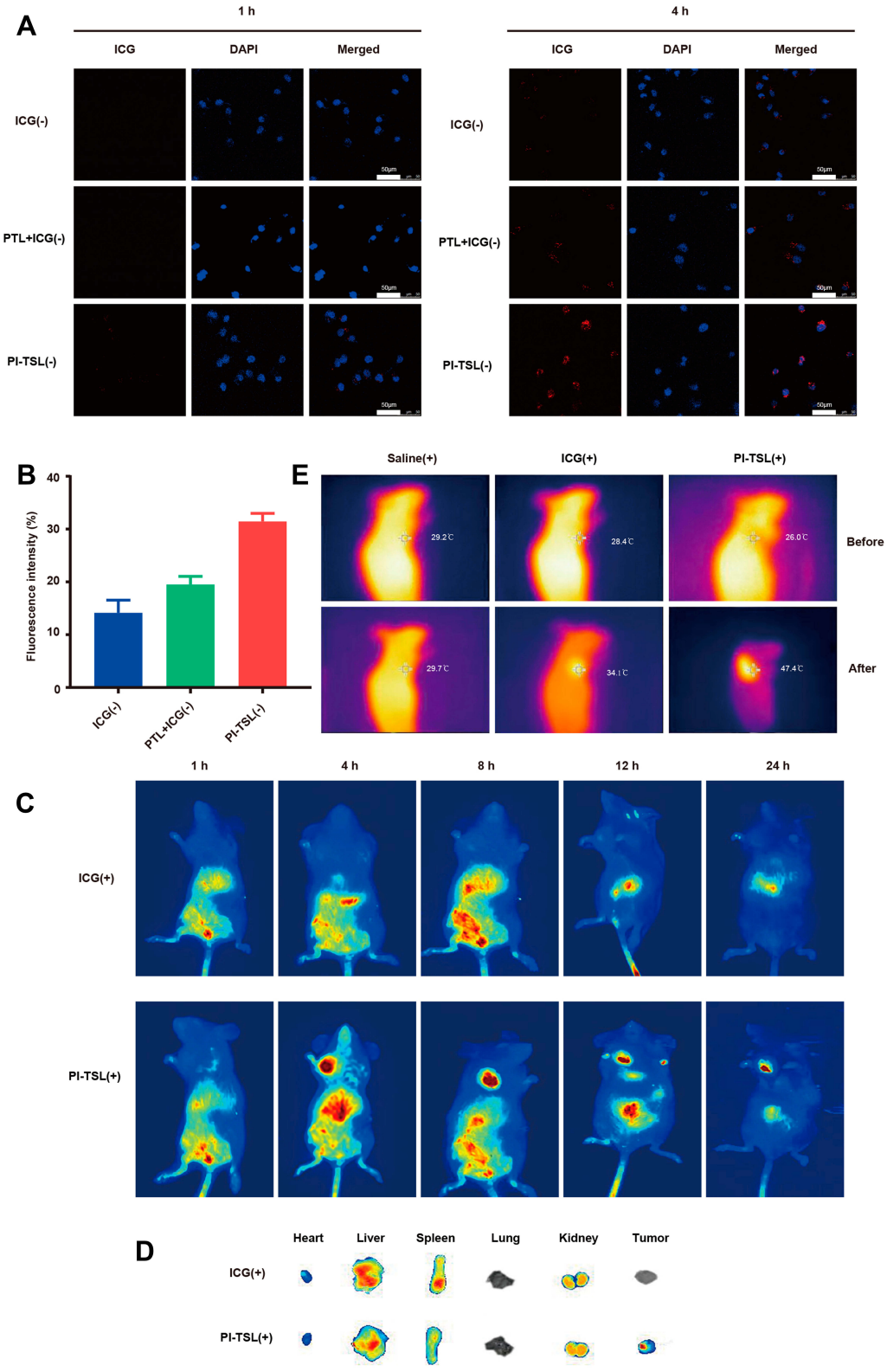

Figure 4 CLSM observation (**A**) of the uptake of ICG (-), PTL+ICG (-), and PI-TSL (-) at 1 and 4 h. Fluorescence quantification (**B**) of uptake at 4 h by flow cytometry. Time-dependent biodistribution (**C**) and major tissue distribution at the end of experiments (**D**) post-injection of ICG (+) or PI-TSL (+) in vivo. Infrared thermography (**E**) of mice intravenously injected with saline (+), ICG (+), or PI-TSL (+) at 8 h after NIR laser stimulation.

Distribution in vivo

In the ICG (+) group with 2 mg/kg ICG, no significant fluorescence distribution in the tumor location within 24 h could be observed (Figure 4C). However, with the equal dose of ICG in the PI-TSL (+) group, the fluorescence signal in tumor tissues increased gradually after an intravenous injection, which peaked at 8 h. Noteworthy, the thermosensitive liposomes are capable of drug-delivery to tumor tissues due to their enhanced permeability and retention (EPR). Furthermore, because of laser stimulation, the PI-TSL (+) released high amounts of loaded drugs at the tumor site. For further verification, major organs were excised at the end of the experiment and observed by fluorescence imaging (Figure 4D). Fluorescence signals in the tumor tissues could be visualized only in the group that was administered with the PI-TSL (+), which was consistent with the fluorescence distribution in vivo.

Photothermal Imaging

As shown in Figure 4C, tumor tissues had the highest concentration of drugs at 8 h after treatment. The highest temperatures in the tumor tissues were observed at 8 h. The maximum temperatures (Figure 4E) recorded were 29.7°C±1.61°C, 34.1°C ±3.11°C, and 47.4°C±2.68°C following treatment with physiological saline, ICG (+), and PI-TSL (+) with an equal dose of 2 mg/kg ICG, respectively. The temperature of the tumor tissues treated with PI-TSL (+) was adequate for the induction of irreversible damage to tumor tissues.[24] The melting temperature of DPPC was 41.3°C, one of the main reasons for triggering the effects by PI-TSL (+).[25] Meanwhile, ICG (+) group exhibited low efficiency with photothermal therapy. The temperature in tumor tissue was 34.1°C±3.11°C. These results coincided with the in vivo distribution results. Furthermore, the results of the in vitro warming experiments (Figure 2D) and in vivo thermography (Figure 4E) show that the PI-TSL (+) could be induced to release heat energy after a near-infrared excitation, to achieve heating of the tumor. The in vitro dissolution experiments (Figure 2C) indicated that PI-TSL (-) was released slowly in normal tissues. After irradiation with a laser, the PI-TSL (+) rapidly released the encapsulated drugs at the tumor site, possibly due to the local warming, and released the drug in response to the near-infrared light, which further enhanced the drug concentration at the tumor site.

Therapeutic Effects of the PI-TSL (+)

As shown in Figure 5A and C, although both the ICG+PTL (-) and the PI-TSL (-) with 30 mg/kg PTL and 2 mg/kg ICG (+) exhibited anti-tumor effects, simple chemotherapy approaches have limitations. When combined with a photothermal and photodynamic therapy, tumor volumes decreased by 42.1% and 58.9% ($P < 0.05$), respectively, after treatment with the same dose of ICG+PTL (+) and PI-TSL (+), when compared to the size in the control. The tumors in mice treated with the PI-TSL (+) showed remarkably limited growth, and demonstrated the best anti-tumor effect. The tumor control rate of PI-TSL (+) with 30 mg/kg PTL and 2 mg/kg ICG (+) was 2.08 times higher than that conferred by the PTX (-) with 10 mg/kg PTX ($P < 0.05$). Furthermore, when compared to the control (Figure 5B), the body weight of mice in the PTX (-) and the PI-TSL (+) groups decreased by 15.5%±1.71% and 3.9%±0.21%, respectively. Immuno-histochemical analysis (Figure 5D and E) of Ki67 expression in tumor tissues indicated the lowest positive proportion in the PI-TSL (+) group ($P < 0.05$), which was only 7.96%±0.85% and validated the results obtained both, in vitro and in vivo. H&E-stained tumor sections (Figure 5F) revealed large areas with apoptotic damage and necrosis in tumor tissues in cells treated with the PI-TSL (+) when compared to that observed in the control and other treatments. H&E staining also revealed that none of the groups exhibited signs of tissue damage in the heart, the liver, the spleen, the lungs, and the kidneys, thereby, demonstrating a low systemic toxicity of our combination therapy (Figure 5G).

The tumor inhibition rate in the PI-TSL (+) group irradiated with a near-infrared light was 2.08-fold higher than that observed in the PTX group (Figure 5A and C) ($P < 0.05$). Changes in body weight (Figure 5B) and H&E staining of major tissues (Figure 5G) of nude mice revealed that PI-TSL (+) and irradiation with the near-infrared light were relatively safe based on the unchanged body weight of the nude mice. Furthermore, no significant toxicity was observed in any organs examined. These results indicate that PI-TSL (+) is a safe and an effective anti-tumor agent for the MDA-MB-231 tumor cell-resembling mouse model.

Discussion

In a previous study, the thermosensitive liposomal formulation of ICG compensated for the phototoxicity at the tumor location, suggesting that thermosensitive liposomes could serve as a delivery platform for ICG in photothermal

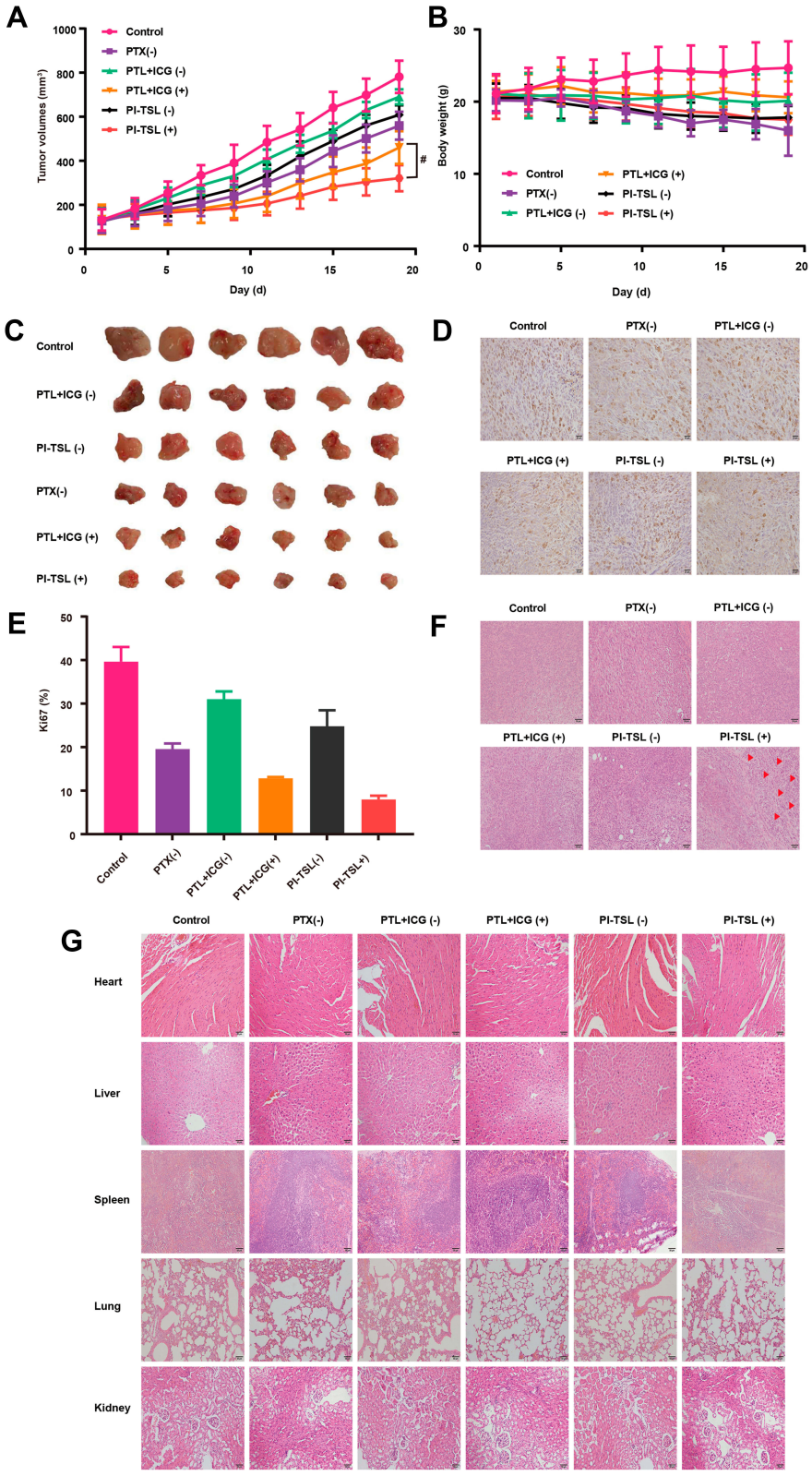

Figure 5 Changes in tumor volume (**A**) and body weight (**B**) of MDA-MB-231 tumor-bearing nude mice in different treatment groups within 19 days. Ex vivo tumor images (**C**) of treated mice on day 19. Ki67 staining (**D**) and its quantitative analysis (**E**) of the excised tumors. Histopathological analysis of the excised tumors (**F**) and major tissues (**G**) by H&E staining. #Stands for P < 0.05 ICG+PTL (+) versus PI-TSL (+); arrow represents apoptotic and necrotic areas.

therapy.[17] Recent studies have shown that photothermally amplified therapeutic liposomes have been developed to synergize cytotoxic chemotherapy or oligonucleotide for an effective cancer treatment.[11,26,27] Although these approaches have helped to enrich the treatment effects, combined administration of non-cytotoxic natural drugs could also achieve better antitumor effects as shown in this study. Non-cytotoxic natural drugs are abundant in different plant-based food items, including fruits and vegetables, and are regularly consumed by humans as a part of their everyday diet. Moreover, due to their long-term consumption, the safety profile of these compounds has been well- established.[28] Our results suggest that the thermosensitive natural products-loaded liposomal ICG may have enormous potential for clinical translation in the treatment of various tumors and these were compatible with laser irradiation as well. Thus, the combination usage of these drugs with a laser irradiation may minimize the adverse treatment effects through synergistic therapeutic effects.

Furthermore, a meta-analysis of 2589 cancer patients showed no significant differences in the objective response rate, overall survival, and progression-free survival between the normal liposome and the conventional chemotherapy groups.[29] The PI-TSL (-) group without a near-infrared excitation behaved like the normal liposomes and exhibited inefficient drug delivery to the target cells leading to ineffective therapy.[30] The key mechanisms of action of PTL are induction of ROS and impairment of MMP. Compared to the PI-TSL (-) group, the PI-TSL (+) has unique advantages, improving the overall therapeutic efficacy. In the case of the PI-TSL (+) group, after reaching the phase transition temperature, the PI-TSL (+) group transition from a colloidal crystal state to a liquid crystal, resulting in an increased fluidity and a better permeation ability. This favors the diffusion of PTL and ICG across the membrane to achieve higher concentrations in the tissues. This also favors the formation of PTL and ICG aggregates at high concentrations at the tumor site. Furthermore, ICG responded to the near-infrared light irradiation at the tumor site by releasing heat energy and combined with PTL induced a more ROS-mediated killing of the tumor cells; thereby, exerting a synergistic effect for treating triple-negative breast cancer. Future studies should, therefore, focus on the optimization of drug dose, ratio and target, and drug delivery performance of the carrier, which can contribute to enhance the therapeutic effects.

Conclusion

In summary, the photothermally-responsive liposomes were successfully prepared to synergize non-cytotoxic PTL and hyperthermia for an effective breast cancer treatment. PI-TSL (+) alone exhibited a greater therapeutic outcome both in vitro and in vivo over chemotherapy and photothermal therapy. Furthermore, several photosensitizers and non-cytotoxic antitumor drugs are available that can be used in the potential treatment for triple-negative breast cancer using different nanocarriers, and this warrants further investigation.

Abbreviations

ICG, indocyanine green; ICG (-), indocyanine green without laser; ICG (+), indocyanine green with laser; PTL, parthenolide; PTL (-), parthenolide without laser; ICG+PTL (-), indocyanine green and parthenolide without laser; ICG+PTL (+), indocyanine green and parthenolide with laser; PI-TSL, indocyanine green-parthenolide thermosensitive liposome; PI-TSL (-), indocyanine green-parthenolide thermosensitive liposome without laser; PI-TSL (+), indocyanine green-parthenolide thermosensitive liposome with laser; PTL-TSL, parthenolide thermosensitive liposome; PTL-TSL (+), parthenolide thermosensitive liposome with laser; PDI, polydispersity index; PTX (-), paclitaxel without laser; TEM, transmission electron microscopy; DAPI, 4′,6-diamidino-2-phenylindole; DPPC, dipalmitoylphosphatidylcholine; DSPC, distearoylphosphatidylcholine; PDI, polydispersity index; FBS, fetal bovine serum; PBS, phosphate-buffered solution; CLSM, confocal laser scanning microscopy; MTT, 3-(4,5-dimethyl-2-thiazolyl)-2,5-diphenyl-2-H-tetrazolium bromide; IC_{50}, half-maximal inhibitory combination value; NIR, near-infrared light response; ROS, reactive oxygen species; MMP, mitochondrial membrane potential; EPR, enhanced permeability and retention; H&E, hematoxylin-eosin staining.

Funding

This work was supported by 333 project of Jiangsu Province (BRA2016258), Medical research project of Jiangsu provincial health commission (H2019096), Jiangsu Youth Medical Talents Project (QNRC2016482) and the Six Talent Peak Projects in Jiangsu Province (WSW-304).

Disclosure

The authors declare that they have no competing interests.

References

1. Siegel RL, Miller KD, Jemal A. Cancer statistics, 2018. *CA Cancer J Clin*. 2018;68:7–30. doi:10.3322/caac.21442
2. Dent R, Trudeau M, Pritchard KI, et al. Triple-negative breast cancer: clinical features and patterns of recurrence. *Clin Cancer Res*. 2007;13:4429–4434. doi:10.1158/1078-0432.CCR-06-3045
3. Lowery AJ, Kell MR, Glynn RW, Kerin MJ, Sweeney KJ. Locoregional recurrence after breast cancer surgery: a systematic review by receptor phenotype. *Breast Cancer Res Treat*. 2012;133:831–841. doi:10.1007/s10549-011-1891-6
4. Adams S, Diamond JR, Hamilton E, et al. Atezolizumab plus nab-paclitaxel in the treatment of metastatic triple-negative breast cancer with 2-year survival follow-up: a phase 1b clinical trial. *JAMA Oncol*. 2019;5(3):334–342. doi:10.1001/jamaoncol.2018.5152
5. Schmid P, Adams S, Rugo HS, et al. Atezolizumab and nab-paclitaxel in advanced triple-negative breast cancer. *N Engl J Med*. 2018;379 (22):2108–2121. doi:10.1056/NEJMoa1809615
6. Lee J, Yesilkanal AE, Wynne JP, et al. Effective breast cancer combination therapy targeting BACH1 and mitochondrial metabolism. *Nature*. 2019;568:254–258. doi:10.1038/s41586-019-1005-x
7. Yamamoto T, Kanaya N, Somlo G, Chen S. Synergistic anti-cancer activity of CDK4/6 inhibitor palbociclib and dual mTOR kinase inhibitor MLN0128 in pRb-expressing ER-negative breast cancer. *Breast Cancer Res Treat*. 2019;174:615–625. doi:10.1007/s10549-018-05104-9
8. Pawar A, Prabhu PP. Nanosoldiers: a promising strategy to combat triple-negative breast cancer. *Biomed Pharmacother*. 2019;110:319–341. doi:10.1016/j.biopha.2018.11.122
9. Reinhart MB, Huntington CR, Blair LJ, Heniford BT, Augenstein VA. Indocyanine green: historical context, current applications, and future considerations. *Surg Innov*. 2016;23:166–175. doi:10.1177/1553350615604053
10. Zhang H, Zhang X, Zhu X, et al. NIR light-induced tumor phototherapy using photo-stable ICG delivery system based on inorganic hybrid. *Nanomedicine*. 2018;14:73–84. doi:10.1016/j.nano.2017.08.019
11. Dai Y, Su J, Wu K, et al. Multifunctional thermosensitive liposomes based on natural phase-change material: near-infrared light-triggered drug release and multimodal imaging-guided cancer combination therapy. *ACS Appl Mater Interfaces*. 2019;11:10540–10553. doi:10.1021/acsami.8b22748
12. Ye H, Wang K, Wang M, et al. Bioinspired nanoplatelets for chemo-photothermal therapy of breast cancer metastasis inhibition. *Biomaterials*. 2019;206:1–12. doi:10.1016/j.biomaterials.2019.03.024
13. Lee YH, Ma YT. Synthesis, characterization, and biological verification of anti-HER2 indocyanine green-doxorubicin-loaded polyethyleneimine-coated perfluorocarbon double nanoemulsions for targeted photochemotherapy of breast cancer cells. *J Nanobiotechnol*. 2017;15:41. doi:10.1186/s12951-017-0274-5
14. Lin L, Liang X, Xu Y, Yang Y, Li X, Dai Z. Doxorubicin and indocyanine green loaded hybrid bicelles for fluorescence imaging guided synergetic chemo/photothermal therapy. *Bioconjug Chem*. 2017;28:2410–2419. doi:10.1021/acs.bioconjchem.7b00407
15. Ghantous A, Sinjab A, Herceg Z, Darwiche N. Parthenolide: from plant shoots to cancer roots. *Drug Discov Today*. 2013;18:894–905. doi:10.1016/j.drudis.2013.05.005
16. Ge W, Hao X, Han F, et al. Synthesis and structure–activity relationship studies of parthenolide derivatives as potential anti-triple-negative breast cancer agents. *Eur J Med Chem*. 2019;166:445–469. doi:10.1016/j.ejmech.2019.01.058
17. Shemesh CS, Moshkelani D, Zhang H. Thermosensitive liposome formulated indocyanine green for near-infrared triggered photodynamic therapy: in vivo evaluation for triple-negative breast cancer. *Pharm Res*. 2015;32:1604–1614. doi:10.1007/s11095-014-1560-7
18. Shi M, Anantha M, Wehbe M, et al. Liposomal formulations of carboplatin injected by convection-enhanced delivery increases the median survival time of F98 glioma-bearing rats. *J Nanobiotechnol*. 2018;16:77. doi:10.1186/s12951-018-0404-8
19. Zhu S, Luo F, Li J, Zhu B, Wang GX. Biocompatibility assessment of single-walled carbon nanotubes using *Saccharomyces cerevisiae* as a model organism. *J Nanobiotechnol*. 2018;16:44. doi:10.1186/s12951-018-0370-1
20. Zhu F, Tan G, Zhong Y, et al. Smart nanoplatform for sequential drug release and enhanced chemo-thermal effect of dual drug loaded gold nanorod vesicles for cancer therapy. *J Nanobiotechnol*. 2019;17:44. doi:10.1186/s12951-019-0473-3
21. Jafari N, Nazeri S, Enferadi ST. Parthenolide reduces metastasis by inhibition of vimentin expression and induces apoptosis by suppression elongation factor α - 1 expression. *Phytomedicine*. 2018;41:67–73.25. doi:10.1016/j.phymed.2018.01.022
22. Wen J, You KR, Lee SY, Song CH, Kim DG. Oxidative stress-mediated apoptosis. The anticancer effect of the sesquiterpene lactone parthenolide. *J Biol Chem*. 2002;277(41):38954–38964. doi:10.1074/jbc.M203842200
23. Jin X, Li M, Yin L, Zhou J, Zhang Z, Lv H. Tyroservatide-TPGS-paclitaxel liposomes: tyroservatide as a targeting ligand for improving breast cancer treatment. *Nanomedicine*. 2017;13(3):1105–1115. doi:10.1016/j.nano.2016.10.017
24. Issels RD. Hyperthermia adds to chemotherapy. *Eur J Cancer*. 2008;44:2546–2554. doi:10.1016/j.ejca.2008.07.038
25. Kitano T, Onoue T, Yamauchi K. Archaeal lipids forming a low energy-surface on air-water interface. *Chem Phys Lipids*. 2003;126:225–232. doi:10.1016/j.chemphyslip.2003.08.006
26. Yoon HJ, Lee HS, Jung JH, Kim HK, Park JH. Photothermally amplified therapeutic liposomes for effective combination treatment of cancer. *ACS Appl Mater Interfaces*. 2018;10(7):6118–6123. doi:10.1021/acsami.7b15996
27. Kontturi LS, van den Dikkenberg J, Urtti A, Hennink WE, Mastrobattista E. Light-triggered cellular delivery of oligonucleotides. *Pharmaceutics*. 2019;11(2):E90. doi:10.3390/pharmaceutics11020090.
28. Kashyap D, Tuli HS, Yerer MB, et al. Natural product-based nanoformulations for cancer therapy: opportunities and challenges. *Semin Cancer Biol*. 2019;S1044-579X(19)30103–8
29. Petersen GH, Alzghari SK, Chee W, Sankari SS, La-Beck NM. Meta-analysis of clinical and preclinical studies comparing the anticancer efficacy of liposomal versus conventional non-liposomal doxorubicin. *J Control Release*. 2016;232:255–264. doi:10.1016/j.jconrel.2016.04.028
30. Abri Aghdam M, Bagheri R, Mosafer J, et al. Recent advances on thermosensitive and pH-sensitive liposomes employed in controlled release. *J Control Release*. 2019;315:1–22. doi: 10.1016/j.jconrel.2019.09.018